Vol 11 No 11, November 2002
1009-1963/2002/11(11)/1145-04

Chinese Physics

© 2002 Chin. Phys. Soc.
and IOP Publishing Ltd

A method of detecting capture γ-rays in a strong pulsed radiation field

Xu Rong-Kun(徐荣昆), Tang Zheng-Yuan(唐正元), and He Xi-Jun(何锡钧)

China Academy of Engineering Physics, Mianyang 621900, *China*

(Received 3 December 2001; revised manuscript received 16 July 2002)

We present a technology for diagnosing the D–T fusion process by detecting capture γ-rays. This technology provides an alternative route to diagnosing the D–T reaction process when a great deal of heavy Z materials surrounds the D–T region. A very important aspect of this paper is to focus on the methods of shielding low-energy γ-rays whose radiation intensity is 10^6 times higher than that of the capture γ-rays. Another aspect is about how to distinguish signal from noise. The result of a 50/1 signal-to-noise ratio indicates that the designed double-magnetic spectrograph is very successful for diagnosing the D–T fusion reaction process.

Keywords: prompt physical process diagnostic, D–T fusion, capture γ-rays, strong pulsed radiation field

PACC: 2570J, 2930K, 0670D

1. Introduction

There are many papers containing reports on the experimental technology of detecting the 16.7MeV γ-rays released by D–T fusion. A prevailing concept in the investigation of fusion considers that we can understand the reaction process with the aid of the characteristic parameters of the 16.7MeV γ-rays. However, when a great deal of high atomic number (Z) material such as ^{238}U surrounds the D–T reaction region, it gives large attenuation to the 16.7MeV emerging γ-rays due to large optic thickness. On the other hand, the fusion neutron with a mean energy of 14.1MeV is captured by the high Z material, which will promptly radiate the so-called capture γ-rays with higher energy than that of the neutron. In fact, the intensity of the leaking capture γ-rays will be much higher than that of the leaking 16.7MeV γ-rays since the capture γ-rays produced in the outer layer can easily penetrate the material. In addition, there will be little difference in rise time between the capture γ-rays and the D–T fusion reaction due to the very short flying distance of the neutrons penetrating the materials. So in this situation, it is good to choose that the D–T reaction process is diagnosed by detecting the capture γ-rays released.

A great difficulty in detecting capture γ-rays lies in the strong interference of the low-energy γ-rays produced by fission and non-elastic scattering, which emerge in the process of the neutron penetrating the surrounding materials. So, one of the key techniques introduced in this paper is to shield this disturbance to increase the signal-to-noise (S/N) ratio.

2. Detecting system

In view of the particular situation that the capture γ-rays are detected in a strong radiation field of low-energy γ-rays, whose original intensity coming out of surrounding materials is about 10^6 times higher than that of the capture γ-rays, we have developed three sets of one-dimension-focus double-magnetic spectrograph (DMS) with peak responses to 16.5MeV, 17.5MeV, and 18.5MeV, respectively. Each of these incorporates a collimator or slit, flight pipes, a Be foil target, first and second magnetic analysers, a detector, a long cable and a recording system. The working principle is as follows.

The collimated capture γ-rays enter the DMS after several tens of meters of flight. There is a beryllium target in the spectrometer which converts capture γ-rays to electrons with energy slightly lower than that of the γ-rays. The electrons come out of the target and fly within a small angle into the first magnetic analyser located 30 cm behind the target through a slit. The magnetic analyser selects electrons with certain

energies and directs them to enter the second magnetic analyser. After the flight electrons are again filtered, the electrons originally converted by capture γ-rays are transformed to electric signals by a detector and recorded by an oscilloscope via a long co-axial cable. Figure 1 shows the schematic diagram of the DMS.

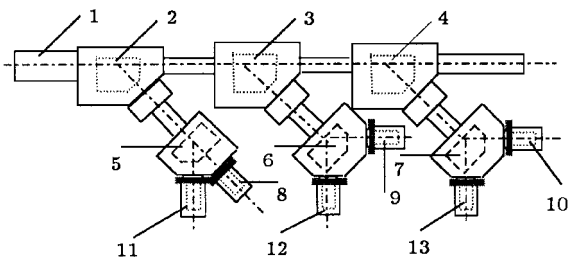


Fig.1. Schematic diagram of the DMS: 1 is the main-pipe; 2, 3, 4, 5, 6, and 7 are the magnetic analysers; 8, 9, and 13 are $1^\sharp$, $2^\sharp$, and $3^\sharp$ background-detectors, respectively; 10, 11, and 12 are $3^\sharp$, $1^\sharp$, and $2^\sharp$ signal-detectors, respectively.

Because the detectors are sensitive to the electrons originally produced by both capture γ-rays and low-energy γ-rays, in order to obtain usable data with high S/N ratio, it is necessary first of all to reduce the intensity of the low-energy γ-rays reaching the DMS. Two methods are adopted.

Firstly according to the difference of the reaction regions between capture γ-rays and low-energy γ-rays, a collimator was set up in the incident port of the main pipe, and the collimator aperture was selected to allow most of the emitted capture γ-rays to be viewed by the target, but only a small fraction of material which emits low-energy γ-rays could be observed. Calculation by a numerical modelling shows that this method is very effective in reducing the noise level.

Secondly, because $(CH_2)_n$ has a low mass-absorption coefficient for capture γ-rays and a high mass-absorption-coefficient for low-energy γ-rays, which can effectively prevent the low-energy γ-rays from reaching the DMS, we put a length of 40cm of this type of material in the flight pipe, which gives 1/10 attenuation to the low-energy γ-rays but only about 1/2 to the capture γ-rays. Using this method, the disturbance level is about five times repressed.

In order to eliminate the disturbance of neutrons released by the fusion, a flight pipe about 10 m length was designed. This pipe makes the DMS unaffected within 140 ns after the capture γ-rays reach.

The intensity of the low-energy γ-rays are 10^4 times higher in intensity than the capture γ-rays reaching the target after the application of the above two methods. More set-ups must be adopted. We firstly mounted a collimator, with a 40 cm length, 40 cm$\times$40 cm area and ϕ25 mm inner aperture, in the incident port of the DMS, which efficiently restricts the low-energy γ-rays entering the immediate DMS and protects the inner wall of the main pipe and the magnet's N–S pole from being directly irradiated. In addition to this, we also place enough bulk lead surrounding the main pipe and the detectors to make the low-energy γ-rays, scattered by the targets and by the inner wall of the main pipe, reach the position of the detectors only along the electron-flying-path after a second scattering and later a third scattering by the inner wall of the first magnetic analyser and by the second magnetic analyser successively. In order to enhance the reliability of shielding of low-energy γ-rays coming from the first scattering of the target and from the second scattering of the inner wall of the main pipe, we also placed enough lead of width 16 cm between the main pipe and the detector. This setting attenuated the γ-rays 10^5 times before reaching the detector.

As confirmed by the experiment, all of above shielding settings are valid and make the background detectors have low noise level. The fact that the three sets of DMS all have high S/N ratio provides a key evidence that the output of the signal detectors is indeed contributed by electrons induced by the expected high-energy γ-rays.

Whether the output currents of the signal detectors are indeed induced by captured γ-rays is very important for evaluating the system's validity. As shown in Fig.1, the background level in the detecting system is monitored in different manners. The $2^\sharp$ and $3^\sharp$ background detectors are placed in the same way as the $3^\sharp$ and $2^\sharp$ signal detectors, respectively, and they are also at the same distance from the main pipe. In addition, the $1^\sharp$ background detector is placed in the direction leading from the first magnetic analyser to the second, so the $1^\sharp$ background detector can keep watch on the maximal background level, and the $2^\sharp$ and $3^\sharp$ background detectors can keep watch on the same background environment as the $3^\sharp$ and $2^\sharp$ signal detectors, respectively. Thus we can obtain a comprehensive evaluation of the noise level in the detector's output.

In addition to monitoring the background level, we also used two specific detectors placed behind the DMS to directly measure the characteristic parameters of the low-energy γ-rays. By comparing the dif-

ference of the characteristic parameters between capture γ-rays and low-energy γ-rays, we provide further experimental evidence that the rise time τ_r and the full width at half maximum (FWHM) of the former are much smaller than the latter, and this once more confirms the authenticity of the system.

3. Related calibrations

3.1. The calibration of electron flight orbit

The most important calibration is to make the electrons induced by the capture γ-rays fly along an expected orbit from the target to the signal detector. This was done by using an electron source of a recycle accelerator (Fig.2). The incident intensity of the electron source was monitored by a Faraday cup, and the electron intensity out of the second magnetic analyser was detected by a scintillation detector. The correct electron flight path was obtained by adjusting the magnet field of the first and second analysers.

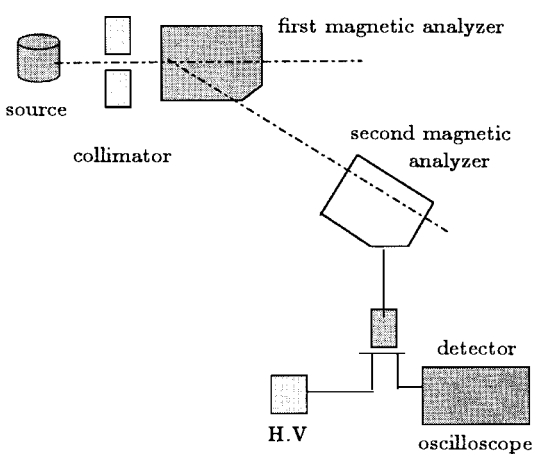


Fig.2. Schematic diagram of the electron orbit calibration.

Multiple energies were used in the calibration. Table 1 shows the results of a certain DMS. As seen from the table, the system has a maximal response at about 17.5MeV. This result is consistent with simulated conclusion of a numerical modelling code which can trace the trajectories of electrons out of the target and calculate the energy resolution curve. A resolution of 0.5MeV was obtained by computation.

Table 1. A DMS with a peak response at about 17.5 MeV.

Electron energy/MeV	15.3	16.2	17.2	18.1
Output current/mV	< 10	50	1400	< 10

3.2. The calibration of time response

The time response of the whole system is mainly determined by the detector and the long cable, and the effect of the oscilloscope can be neglected. We first measured the contributions of the detector and the cable separately, and then convoluted them to obtain the time response of the system.

The characteristic parameter τ_r and FWHM of the cable time response were improved by mounting a three-pole-zero-pairs equalizer which makes the whole transmission system have a flat frequency response from about 0 to 300MHz.

The detector's contribution to the whole time response was measured by using a hard x-ray pulsed source with 200ps FWHM; a cable about 10 m in length connects the detector with oscilloscope in this experiment. Figure 3 shows the result.

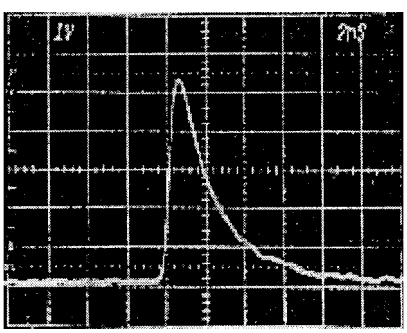


Fig.3. The detector's time response detected by using a pulsed hard x-ray source with 200ps FWHM.

4. The experimental results

All expected data including the separate signal and background information of the three systems were successfully obtained. Figure 4 shows a recorded photograph corresponding to the 17.5MeV capture γ-rays, and Fig.5 shows the maximal disturbance level from the $1^\sharp$ background detector.

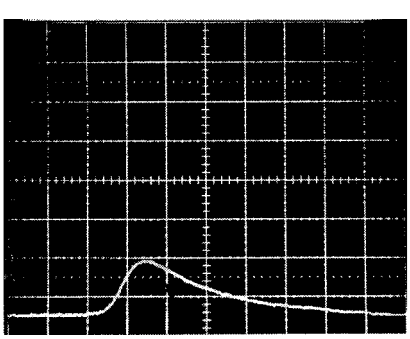


Fig.4. A recorded photograph corresponding to 17.5MeV capture γ-rays from the $2^\sharp$ signal detector.

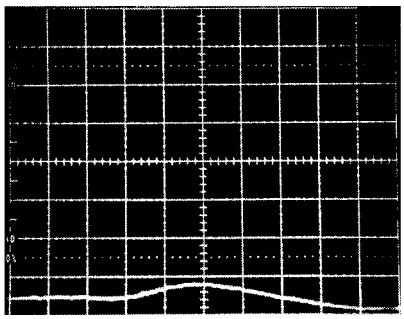


Fig.5. The maximal interference output from the 1♯ background detector.

Many useful parameters are obtained by analysing the current waveforms and amplitude of the capture γ-rays detected, these results provide an insight into the D–T fusion process. Here we only discuss some conclusions about the experiment itself and about certain properties of capture γ-rays.

(i) The S/N ratio in this experiment is 50/1 by comparing the output current of the signal detectors and background detectors. This result suggests that the methods employed to suppress the interference of the low-energy γ-rays are valid. It also shows that the success of shielding low-energy γ-rays is primarily attributed to the set-up of placing a collimator near the source region and to the $(CH_2)_n$ material mounted in the flight pipe.

(ii) The signal's characteristic parameter τ_r and FWHM are much shorter than that of low-energy γ-rays detected by a specific detector. This result again confirms that the signals from signal detectors are not induced by low-energy γ-rays but by capture γ-rays.

(iii) The relative radiation intensity of capture γ-rays out of a material with a high atomic number is inferred by analysing the output current of each detecting system and the corresponding experimental parameters utilized. We obtained that the relative radiation intensities of 16.5MeV, 17.5MeV and 18.5MeV capture γ-rays are 1, 0.67 and 0.40, respectively. This result is consistent with the computation using a numerical modelling code and with simple theoretical analysis, as long as the 16.7MeV γ-rays directly released from D–T fusion are also included in the system of detecting the capture γ-rays with 16.5MeV centre energy and $\pm$0.5MeV resolution.

5. Conclusion

Unlike the prevailing experimental technologies designed for diagnosing the D–T fusion process, the D–T fusion process can also be diagnosed by detecting the characteristic parameters of the capture γ-rays when a great deal of high Z material surrounds the fusion fuel. There is little difference in rising time between capture γ-rays and D–T fusion because of the very short flying distance of the neutron penetrating the material. Many methods have been used for shielding the interference from the low-energy γ-rays, which are 10^6 times stronger in intensity than that of capture γ-rays. These measures being taken, the technology introduced in this paper can successfully detect the capture γ-rays with energies of 16.5MeV, 17.5MeV, 18.5MeV amidst a strong pulsed radiation field and can obtain a high S/N ratio.

Acknowledgments

We thank Hu Ren-yu, Zhou Guo-xiang, Cheng Han-de and all crews of our team for many useful discussions and suggestions. The China Academy of Engineering Physics supported this research.

References

[1] Brolley J E *et al* 1983 *Gas Cerenkov Detector for Measuring* 16.7-MeV *gamma Rays from the D(T,gamma)^{5}He Reaction, LLNL, LA-UR*-83- 1864

[2] Petrrasso R D *et al* Gamma-Rays Diagnostics for the Compact Ignition Tokamak, PFC/JA-88-17

[3] Ladish J S *et al* Obervation of the 16.7MeV Fusion Gamma Using a Gas Cerenkov Detector, LLNL, LA-UR-85-3674

[4] Lerche R A *et al* Fast Pb-neutron-to-light converter for ICF target burn history measurement, LLNL, URCL-JC-103281

[5] Medley S S and Hendel H, Fusion gamma Diagnostics for D–T and D–^{3}He Plasmas, PPPL-1950